

# BPnP: Further Empowering End-to-End Learning with Back-Propagatable Geometric Optimization

Bo Chen, Tat-Jun Chin

School of Computer Science, The University of Adelaide  
Adelaide, South Australia, 5005, Australia

{bo.chen, tat-jun.chin}@adelaide.edu.au

Nan Li

College of Mathematics and Statistics, Shenzhen University  
Shenzhen, 518060, China

nan.li@szu.edu.cn

## Abstract

In this paper we present BPnP, a novel method to do back-propagation through a PnP solver. We show that the gradients of such geometric optimization process can be computed using the Implicit Function Theorem as if it is differentiable. Furthermore, we develop a residual-conformity trick to make end-to-end pose regression using BPnP smooth and stable. We also propose a “march in formation” algorithm which successfully uses BPnP for key-point regression.

Our invention opens a door to vast possibilities. The ability to incorporate geometric optimization in end-to-end learning will greatly boost its power and promote innovations in various computer vision tasks.

## 1. Introduction

In learning problems, often times geometric errors can not be directly used to guide the training. For example, let  $h(\cdot; \theta)$  be a regression model which predicts some 2D key-point locations  $\mathbf{x}$  with input  $I$  and trainable parameters  $\theta$ , i.e.,

$$\mathbf{x} = h(I; \theta), \quad (1)$$

let  $g$  be a PnP solver, which computes the 6DOF camera pose  $\mathbf{y}$  using the 2D keypoint locations  $\mathbf{x}$ , the corresponding 3D coordinates of the structural keypoint expressed in the world frame  $M$  and the camera intrinsic matrix  $K$ , i.e.,

$$\mathbf{y} = g(\mathbf{x}, M, K). \quad (2)$$

For simplicity we omit the input  $M$  and  $K$  and use

$$\mathbf{y} = g(\mathbf{x}) \quad (3)$$

for the rest of the paper. Finally, let  $l(\cdot)$  be a loss function which computes the loss  $\ell$  of the estimated pose  $\mathbf{y}$

$$\ell = l(\mathbf{y}). \quad (4)$$

A typical training scheme is to train the regression model  $h$  by updating  $\theta$  using gradients

$$\frac{\partial \ell}{\partial \theta} = \frac{\partial \ell}{\partial \mathbf{y}} \frac{\partial \mathbf{y}}{\partial \mathbf{x}} \frac{\partial \mathbf{x}}{\partial \theta}. \quad (5)$$

However, the problem of such scheme is that a PnP solver is an optimization process, not simply a continuous or differentiable function. In other words we do not have a way to compute  $\frac{\partial \mathbf{y}}{\partial \mathbf{x}}$  in Equation 5.

To fill this gap, we introduce the Back-propagatable PnP (BPnP), the first ever method that is able to back-propagate through a geometric optimization process using implicit gradients.

## 2. BPnP: the back-propagatable PnP with implicit gradients

In this section we describe step by step how BPnP is created.

### 2.1. The implicit function theorem

**Theorem 1** Let  $f : \mathbb{R}^{n+m} \rightarrow \mathbb{R}^m$  be a continuous differentiable function, which has input  $(\mathbf{x}, \mathbf{y})$  where  $\mathbf{x} \in \mathbb{R}^n$  and  $\mathbf{y} \in \mathbb{R}^m$ . For a point  $(\mathbf{x}_0, \mathbf{y}_0)$ , if

$$f(\mathbf{x}_0, \mathbf{y}_0) = \mathbf{0} \quad (6)$$

and the Jacobian matrix  $\frac{\partial f}{\partial \mathbf{y}}(\mathbf{x}_0, \mathbf{y}_0)$  is invertible, then there exists an open set  $U \subset \mathbb{R}^n$  such that  $\mathbf{x}_0 \in U$  and an function  $g : \mathbb{R}^n \rightarrow \mathbb{R}^m$  such that  $\mathbf{y}_0 = g(\mathbf{x}_0)$  and

$$f(\mathbf{x}', g(\mathbf{x}')) = \mathbf{0}, \forall \mathbf{x}' \in U. \quad (7)$$

Moreover, the Jacobian matrix  $\frac{\partial g}{\partial \mathbf{x}}(\mathbf{x}')$  is given by

$$\frac{\partial g}{\partial \mathbf{x}}(\mathbf{x}') = - \left[ \frac{\partial f}{\partial \mathbf{y}}(\mathbf{x}', g(\mathbf{x}')) \right]^{-1} \left[ \frac{\partial f}{\partial \mathbf{x}}(\mathbf{x}', g(\mathbf{x}')) \right], \quad \forall \mathbf{x}' \in U. \quad (8)$$

For a function  $g(\mathbf{x})$ , the implicit function theorem provides a way of computing the derivatives of  $g$  with respect to  $\mathbf{x}$  without knowing the explicit form of the function, given that  $\mathbf{x}$  and  $g(\mathbf{x})$  are constrained by an function  $f$ . Note that Equation 6 can be relaxed to

$$f(\mathbf{x}_0, \mathbf{y}_0) = \mathbf{c}, \quad (9)$$

where  $\mathbf{c}$  is a constant vector that does not depend on  $\mathbf{x}_0$  or  $\mathbf{y}_0$ . Because for each such  $f$  there exists  $f' = f - \mathbf{c}$  which satisfies Equation 6 and  $\frac{\partial f}{\partial \mathbf{x}} = \frac{\partial f'}{\partial \mathbf{x}}, \frac{\partial f}{\partial \mathbf{y}} = \frac{\partial f'}{\partial \mathbf{y}}$ .

## 2.2. Constructing the constraint function $f$

To utilize the implicit function theorem, we first need to construct the constraint function  $f$  such that  $f(\mathbf{x}, \mathbf{y}) = \mathbf{c}$ . Recall here  $\mathbf{x}$  is the 2D keypoint locations and  $\mathbf{y}$  is the camera pose, a natural idea is to utilize the projection error for constructing  $f$ .

Let  $E(\mathbf{y})$  denote the extrinsic matrix defined by pose  $\mathbf{y}$  and  $P = KE(\mathbf{y})$  denote the 3-by-4 projection matrix. For the  $i$ -th keypoint, the projection equation can be established as

$$\begin{bmatrix} u_i \\ v_i \\ w_i \end{bmatrix} = P \begin{bmatrix} x_i \\ y_i \\ z_i \\ 1 \end{bmatrix}, \quad (10)$$

where  $x_i, y_i$  and  $z_i$  are the 3D coordinates of the  $i$ -th keypoint obtained from  $M$  and its projected 2D coordinates in the image plane can be derived by  $u_i/w_i, v_i/w_i$ . Let  $\mathbf{x}_i = [x_{i,1}, x_{i,2}]^T$  denote the 2D image coordinates of keypoint  $i$  provided by  $\mathbf{x}$ , we defined the residual  $\mathbf{r}_i$  as

$$\mathbf{r}_i = w_i \mathbf{x}_i - \begin{bmatrix} u_i \\ v_i \end{bmatrix}. \quad (11)$$

The above definition of residual is numerically more stable than using  $w_i$  as a denominator.

For  $j = 1, \dots, m$ , define  $f_j$  as

$$f_j = \sum_{i=1}^n C_{j,i} \mathbf{r}_i, \quad (12)$$

where each  $C_{j,i}$  is a 1-by-2 vector of Gaussian random numbers, for  $j = 1, \dots, m$  and  $i = 1, \dots, n$ . Finally, we construct the function  $f : \mathbb{R}^{2n+m} \rightarrow \mathbb{R}^m$  as

$$f(\mathbf{x}, \mathbf{y}) = [f_1, \dots, f_m]^T. \quad (13)$$

The above defined function has output  $f \in \mathbb{R}^m$  and is differentiable with respect to both  $\mathbf{x}$  and  $\mathbf{y}$ . Thus, the implicit gradients of function  $g$  with respect to  $\mathbf{x}$ , *i.e.*,  $\frac{\partial g}{\partial \mathbf{x}}$ , can be calculated using Equation 8. The number of keypoints  $n$  is arbitrary. The number of dimensions of  $\mathbf{y}$ , *i.e.*,  $m$ , is up to the representation of the rotation part of the pose. For example,  $m = 6$  for axis-angle representation,  $m = 7$  for quaternion representation and  $m = 12$  for rotation matrix representation.

## 2.3. Normalizing the implicit gradients

Because the calculation of the implicit gradients involves an inversion of the Jacobian  $\frac{\partial f}{\partial \mathbf{y}}$ , it can sometimes produces large values, making the gradients unstable for training. To address this issue, we normalize the gradients  $\frac{\partial g}{\partial \mathbf{x}}$  with its Frobenius norm:

$$\frac{\partial g}{\partial \mathbf{x}} \leftarrow \frac{\partial g}{\partial \mathbf{x}} / \left\| \frac{\partial g}{\partial \mathbf{x}} \right\|_F.$$

## 2.4. Implementation note

We find that using the axis-angle representation for the rotation part of the pose works best with BPnP. This is possibly because this way the pose representation has dimensionality  $m = 6$  which equals its degrees of freedom.

When calculating the implicit gradients in the backward pass, the solver  $g$  is treated as a black box. It seems that in the forward pass  $g$  can be any PnP solver. However, contrary to common practice, it is important in this case to choose sensitive solvers over robust ones. Thus for the implementation of  $g$ , we use OpenCV's SOLVEPNP\_ITERATIVE method, which is a Levenberg-Marquardt (LM) optimization for minimizing the sum of squared distances between the 2D keypoints  $\mathbf{x}$  and the projected 3D keypoints. The initial pose for the LM optimization for the first time in a iterative algorithm is obtained using RANSAC; we then use the output pose of the previous iteration as initial pose for all iterations.

In the backward pass, the computation of Equation 8 is implemented using the Pytorch autograd package [1].

## 3. End-to-end learning with BPnP

Given a function  $h$  with input  $I$ , output  $\mathbf{x}$  and trainable parameters  $\theta$ , a typical baseline algorithm to use the BPnP solver  $g$  in optimizing some loss function  $l$  would look like Algorithm 1.

There are two issues with this baseline algorithm: firstly and most importantly, the constraint of Theorem 1 as shown in Equation 9 is not always met when training with Algorithm 1; secondly, if BPnP is used for 2D keypoint regression, *i.e.*, regressing  $\mathbf{x}$ , then the prediction is unlikely to approach the ground truth. We further explain these issues and propose their remedies below.

---

**Algorithm 1** Baseline algorithm

---

```
1: while loss  $\ell$  has not converged do
2:    $\mathbf{x} \leftarrow h(I; \boldsymbol{\theta})$ 
3:    $\mathbf{y} \leftarrow g(\mathbf{x})$ 
4:    $\ell \leftarrow l(\mathbf{y})$ 
5:    $\boldsymbol{\theta} \leftarrow \alpha \frac{\partial \ell}{\partial \boldsymbol{\theta}}$ 
6: end while
```

---

### 3.1. The residual-conformity trick

The key for Algorithm 1 to work smoothly lies in that in each iteration,  $g$  should produce an improved pose  $\mathbf{y}$  using the updated  $\mathbf{x}$ , provided a small enough learning rate  $\alpha$ . However, whether this happens or not, depends on whether Equation 9 is upheld or not while computing  $g(\mathbf{x})$ . The implicit function theorem assumes that  $\mathbf{x}$  and  $g(\mathbf{x})$  are constrained by Equation 9, *i.e.*, in our case the linear combinations of the projection residuals must remain the same. In other words, when  $\mathbf{x}$  changes slightly,  $g(\mathbf{x})$  should change accordingly to keep the residuals unchanged. The problem is that PnP solvers are designed to minimize the projection errors instead of keeping them unchanged. This issue causes the training process to become unstable.

To align the objective of the BPnP solver  $g$  and the objective of maintaining the projection residuals as much as possible in order to uphold Equation 9, we use a residual-conformity trick to boost the stability of the training process. Let  $\pi_{\mathbf{y}}$  be the the projective transformation of 3D points into the image plane with pose  $\mathbf{y}$  and known camera intrinsics, *i.e.*,  $\pi_{\mathbf{y}}(M)$  outputs the projected 2D image coordinates of the 3D points  $M$ . Let  $\mathbb{C}()$  denote an operation that copies and detaches a variable from its computational graph, *i.e.*, any variable after such operation will be treated as a constant when involved in any differentiation. Algorithm 2 describes the training procedure with the residual-conformity trick.

---

**Algorithm 2** Training with residual-conformity trick

---

```
1:  $\mathbf{r}_p \leftarrow \mathbf{0}$ 
2: while loss  $\ell$  has not converged do
3:    $\mathbf{x} \leftarrow h(I; \boldsymbol{\theta})$ 
4:    $\mathbf{y} \leftarrow g(\mathbf{x} - \mathbf{r}_p)$ 
5:    $\ell \leftarrow l(\mathbf{y})$ 
6:    $\boldsymbol{\theta} \leftarrow \alpha \frac{\partial \ell}{\partial \boldsymbol{\theta}}$ 
7:    $\mathbf{r}_p \leftarrow \mathbb{C}(\mathbf{x} - \pi_{\mathbf{y}}(M))$ 
8: end while
```

---

The key difference in Algorithm 2 is that at each iteration the projection residual  $\mathbf{r}_p$  based on the previous pose is subtracted from  $\mathbf{x}$  before passing to  $g$  for computing the current pose. This aligns the objective of the BPnP solver  $g$  and the objective of upholding Equation 9. To see this, recall that  $g$  is an optimization process which seeks to minimize the pro-

jection error. If  $\mathbf{y}$  is the output of  $g(\mathbf{x} - \mathbf{r}_p)$ , it means that  $g$  has done its best efforts to let  $\pi_{\mathbf{y}}(M) \rightarrow \mathbf{x} - \mathbf{r}_p$ , which is equivalent to letting  $\mathbf{x} - \pi_{\mathbf{y}}(M) \rightarrow \mathbf{r}_p$ , *i.e.*, trying to uphold Equation 9.

### 3.2. March in formation

With either Algorithm 1 or 2, BPnP is still not good enough for 2D keypoint regression. Suppose during training the output pose  $\mathbf{y} = g(\mathbf{x})$  has reached ground truth, it is still highly unlikely that  $\mathbf{x}$  equals to  $\pi_{\mathbf{y}}(M)$ . Because the PnP solver does not guarantee 0 projection residuals; it merely outputs the pose with minimum residuals. Define a feasible formation as a formation of  $\mathbf{x}$  that satisfies the following condition:

$$\exists \mathbf{y} \in ST(3) \text{ s.t. } \mathbf{x} = \pi_{\mathbf{y}}(M). \quad (14)$$

A fix to this issue is to encourage  $\mathbf{x}$  to keep a feasible formation during training.

---

**Algorithm 3** March in formation

---

```
1:  $\mathbf{r}_p \leftarrow \mathbf{0}$ 
2: while loss  $\ell$  has not converged do
3:    $\mathbf{x} \leftarrow h(I; \boldsymbol{\theta})$ 
4:    $\mathbf{y} \leftarrow g(\mathbf{x} - \mathbf{r}_p)$ 
5:    $\mathbf{x}' \leftarrow \mathbb{C}(\pi_{\mathbf{y}}(M))$ 
6:    $\ell \leftarrow \beta \|\mathbf{x} - \mathbf{x}'\|_2^2$ 
7:    $\boldsymbol{\theta} \leftarrow \alpha \frac{\partial \ell}{\partial \boldsymbol{\theta}}$ 
8:    $\mathbf{x} \leftarrow h(I; \boldsymbol{\theta})$ 
9:    $\mathbf{r}'_p \leftarrow \mathbb{C}(\mathbf{x} - \mathbf{x}')$ 
10:   $\mathbf{y} \leftarrow g(\mathbf{x} - \mathbf{r}'_p)$ 
11:   $\ell \leftarrow l(\mathbf{y})$ 
12:   $\boldsymbol{\theta} \leftarrow \alpha \frac{\partial \ell}{\partial \boldsymbol{\theta}}$ 
13:   $\mathbf{r}_p \leftarrow \mathbb{C}(\mathbf{x} - \pi_{\mathbf{y}}(M))$ 
14: end while
```

---

Algorithm 3 presents such a training scheme, where line 3-7 are to encourage  $\mathbf{x}$  to maintain a feasible formation by approaching the projection  $\pi_{\mathbf{y}}(M)$ , while line 8-12 are to guide the pose to approach the ground truth. This idea can be intuitively viewed as if  $\mathbf{x}$  is trying to march to the destination while maintaining a certain formation.

## 4. Experiment

To show the effectiveness of BPnP, we conduct experiments in two tasks: pose regression and keypoint regression.

Fix a set of  $n$  keypoints with 3D coordinates  $M$ , the camera intrinsic matrix  $K$  and an arbitrary feasible pose  $\mathbf{y}^*$  as the ground truth pose. We use a modified VGG-11 [2] model as a function  $h$  that outputs the 2D keypoint locations  $\mathbf{x}$ :

$$\mathbf{x} = h(I; \boldsymbol{\theta}) \quad (15)$$

with input  $I$  and parameters  $\theta$ . The final layer of the model is modified to output the coordinates of  $n$  keypoints. The BPnP solver  $g$  is as described in Section 2 which computes the pose

$$\mathbf{y} = g(\mathbf{x}; K, M), \quad (16)$$

and the loss function is defined as

$$l(\mathbf{y}, \mathbf{y}^*) = \ell_R + \ell_T, \quad (17)$$

where

$$\ell_R = (2 \cos^{-1}(|\langle \mathbf{y}_R, \mathbf{y}_R^* \rangle|))^2 \quad (18)$$

is the rotation loss and

$$\ell_T = \|\mathbf{y}_T - \mathbf{y}_T^*\|_2^2 \quad (19)$$

is the translation loss. Here  $\mathbf{y}_R$  is the rotation part of  $\mathbf{y}$  converted to quaternion representation and  $\mathbf{y}_T$  is the translation part of  $\mathbf{y}$ , and similarly for  $\mathbf{y}_R^*$  and  $\mathbf{y}_T^*$ .

### 4.1. Pose regression

We fix the input  $I = \mathbf{1}$  and start training  $h$  using Algorithm 1 and 2 respectively, with learning rate  $\alpha = 0.0005$ .

Figure 1 and 2 provide the pose regression results of 3 different runs with  $n = 4$  keypoints using Algorithm 1 and 2, respectively. They show that BPnP are effective in both algorithms. The implicit gradients are able to reduce the loss to near 0 and guide the model to output a pose close to the ground truth.

Figure 1 and 2 also show the importance of the residual-conformity trick. In Figure 1 the loss curves are bumpy and the pose trajectories are messy because Equation 9 is often violated in Algorithm 1. In contrast, Figure 2 shows smooth loss curves and clean trajectories, verifying the effectiveness of the residual-conformity trick in making the training process stable.

### 4.2. Keypoint regression

We conduct 2 sets of keypoint regression experiments using Algorithm 2 and 3 respectively. Figure 3 and 4 provides the results of the experiments.

Figure 3 demonstrates the issue discussed in Section 3.2: despite that the pose  $\mathbf{y}$  has converged to  $\mathbf{y}^*$ , the output 2D keypoints  $\mathbf{x}$  are still far away from  $\pi_{\mathbf{y}^*}(M)$ . On the other hand, as shown in Figure 4 (c) and (f) both experiments are successful in converging  $\mathbf{x}$  to  $\pi_{\mathbf{y}^*}(M)$ . This proves that the march in formation algorithm can be used for predicting 2D keypoint locations.

## 5. Conclusion

In this paper we present BPnP, a novel method to do back-propagation through a PnP solver. We show that the gradients of such geometric optimization process can

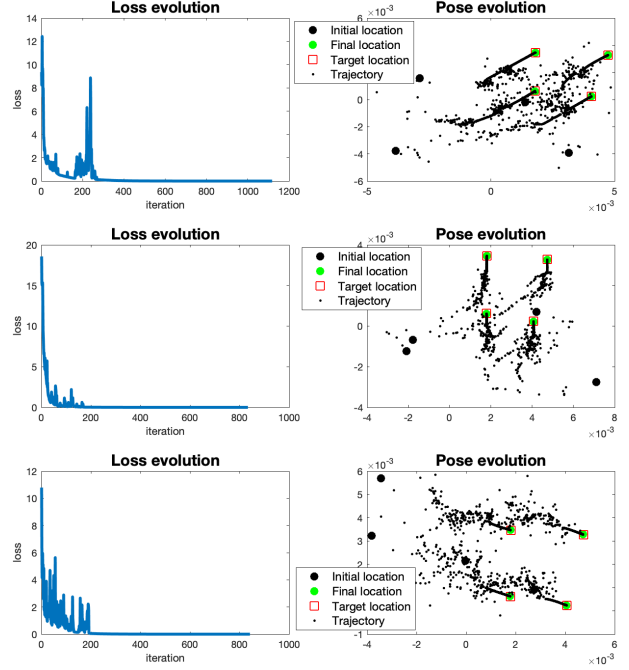


Figure 1. Three different runs using the baseline Algorithm 1. The right-hand-side plots show the trajectory of the 3D keypoints projected using the output pose of the model in each iteration, *i.e.*,  $\pi_{\mathbf{y}}(M)$ . The red square markers are the ground truth pose projection, *i.e.*,  $\pi_{\mathbf{y}^*}(M)$ .

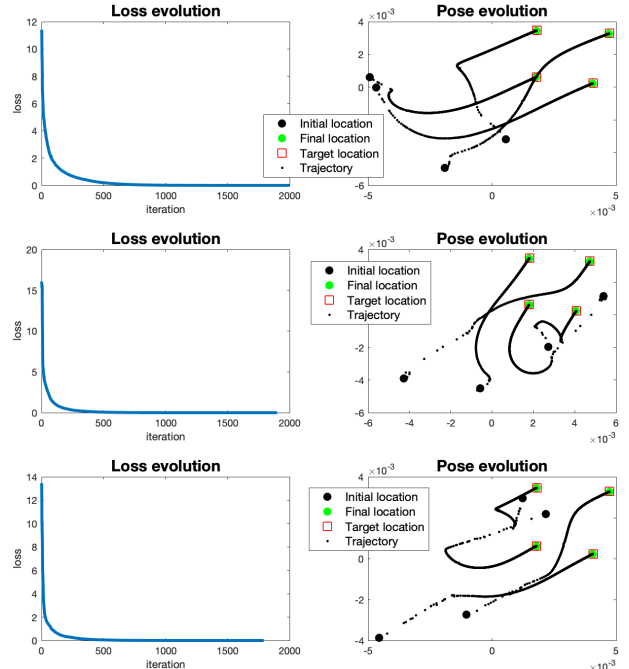


Figure 2. Three different runs using Algorithm 2 with the residual-conformity trick. The meaning of the markers are the same as Figure 1.

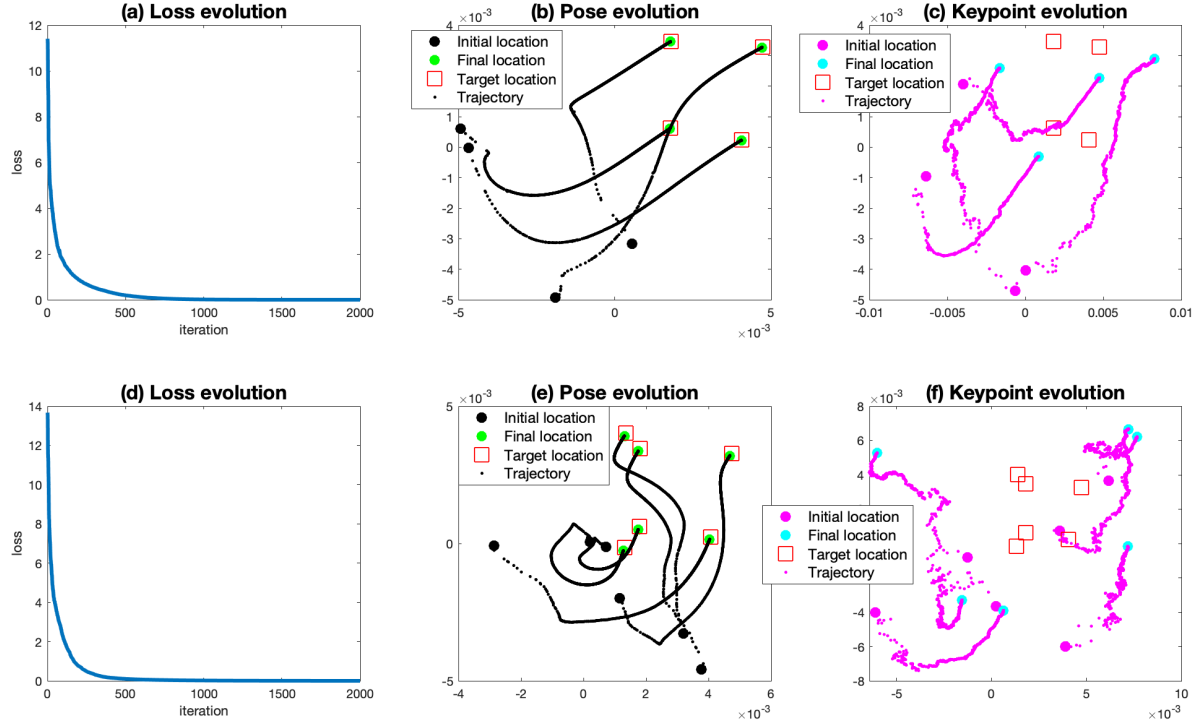


Figure 3. Two different runs using Algorithm 2 with  $n = 4$  and  $n = 6$  keypoints respectively. (b) and (e) are the pose trajectories  $\pi_y(M)$  while (c) and (f) shows the keypoint trajectories  $\mathbf{x}$ . Marker interpretations are same as Figure 1.

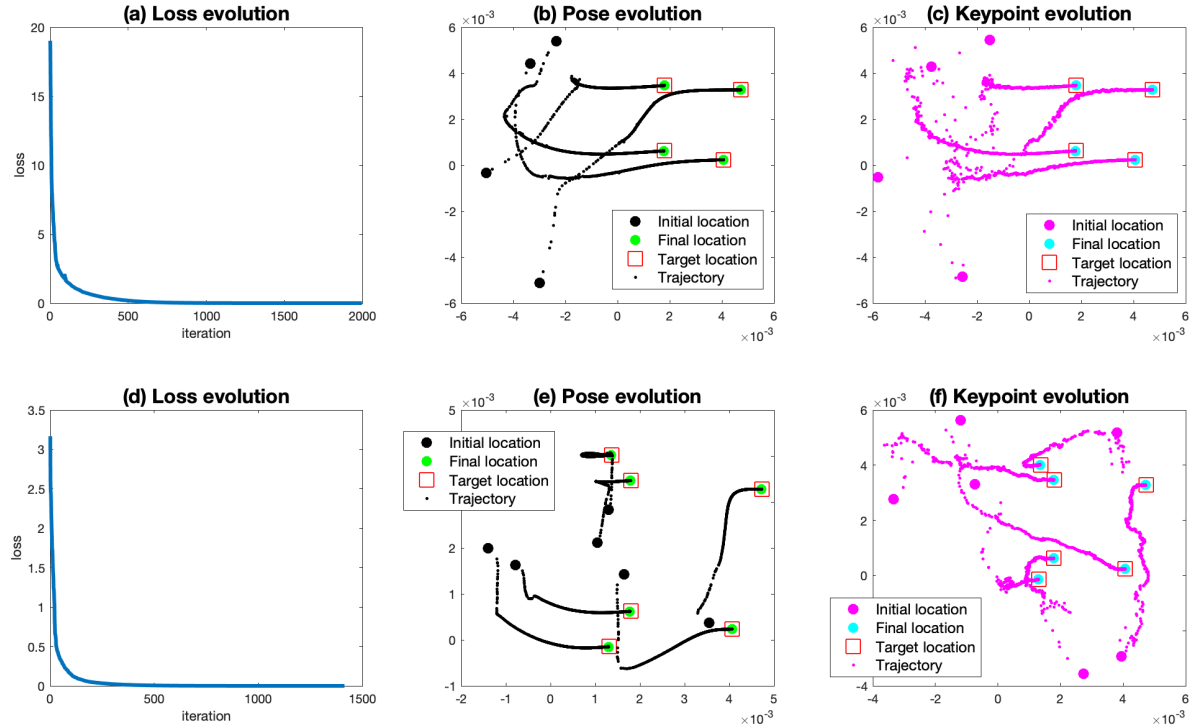


Figure 4. Two different runs using Algorithm 3, march in formation, with  $n = 4$  and  $n = 6$  keypoints respectively. Plot and marker interpretations are same as Figure 3.

be computed using the Implicit Function Theorem as if it is differentiable. Furthermore, we develop a residual-conformity trick to make end-to-end pose regression using BPnP smooth and stable. We also propose a “march in formation” algorithm which successfully uses BPnP for key-point regression.

Our invention opens a door to vast possibilities. The ability to incorporate geometric optimization in end-to-end learning will greatly boost its power and promote innovations in various computer vision tasks.

## References

- [1] Adam Paszke, Sam Gross, Soumith Chintala, Gregory Chanan, Edward Yang, Zachary DeVito, Zeming Lin, Alban Desmaison, Luca Antiga, and Adam Lerer. Automatic differentiation in pytorch. In *NIPS-W*, 2017. 2
- [2] Karen Simonyan and Andrew Zisserman. Very deep convolutional networks for large-scale image recognition. In *ICLR*, 2015. 3